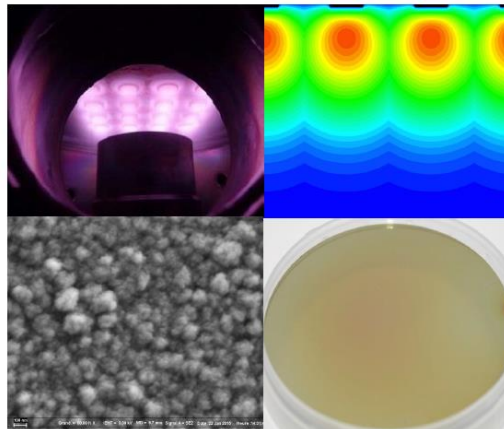


# Characterization of a distributed antenna array microwave plasma used for low-temperature/large-area nanocrystalline diamond film

D. Dekkar<sup>1</sup>, F. Bénédic<sup>1</sup>, X. Aubert<sup>1</sup>, S. Béchu<sup>2</sup>, A. Bès<sup>2</sup>



<sup>1</sup>LSPM-CNRS, Université Paris 13, Sorbonne Paris Cité, Villetaneuse, France

<sup>2</sup>Université Grenoble Alpes, CNRS, Grenoble INP, LPSC-IN2P3, Grenoble, France

# Outline

- Statements
- Experimental plasma diagnostics through :
  - ❖ Langmuir probe
  - ❖ Optical Emission Spectroscopy
- Plasma modelling
- Conclusion

# Diamond properties and applications

## Mechanics

Exceptional mechanical  
**Hardness**  $10^4 \text{kg}\cdot\text{mm}^{-2}$



## Optics

**Optical transparency**  
(Down to 225nm)



## Biomedical

**Biocompatible**

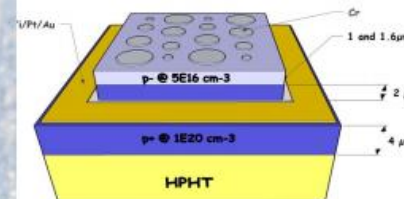
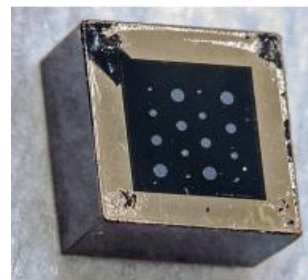


## Electronics

High **Acoustic Velocity** :  $10^4 \text{m}\cdot\text{s}^{-1}$

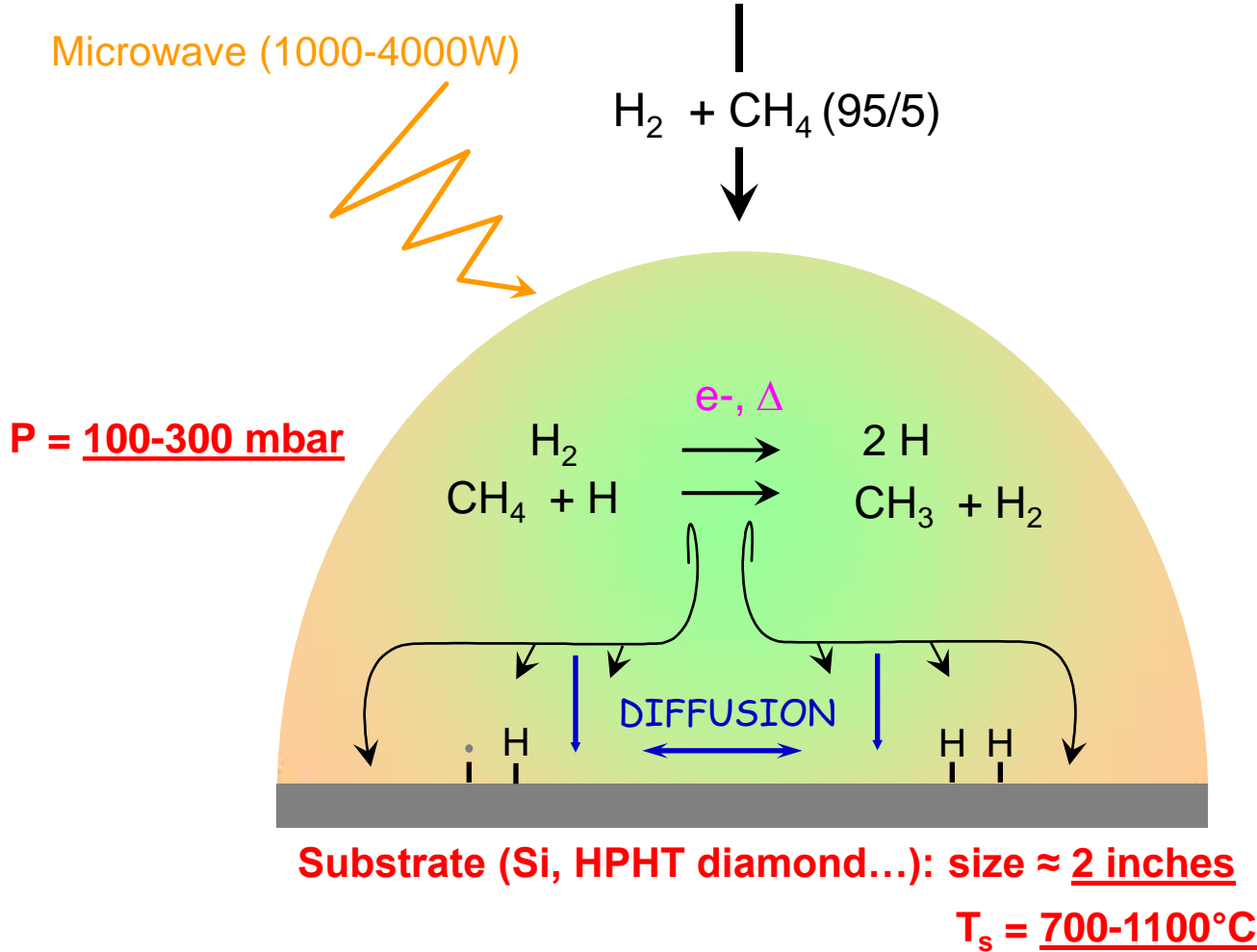


**Wide band gap semiconductor** (5.5 eV)  
**High Thermal Conductivity** (2200 W/mK)



Among various forms of synthetic diamond, **nanocrystalline diamond (NCD) films** possess nanometric grain size and thickness-independent low surface roughness ( $< 20 \text{nm}$ )

# High pressure/high temperature MPACVD process



Development of new applications requires low temperature/large area deposition process

# Distributed antenna array microwave plasma reactor

## The Plasmodie reactor\*



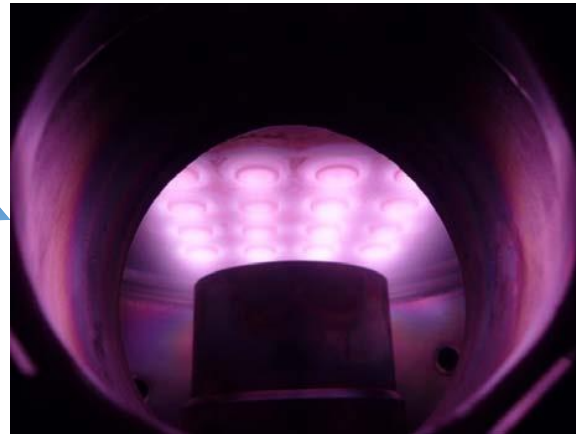
MW Power: 1-3 kW, 2.45GHz

[H<sub>2</sub>]: 90-98 %

[CH<sub>4</sub>]: 1-5 %

[CO<sub>2</sub>]: 1-5 %

Pressure: < 1 mbar



16 coaxial plasma sources arranged in **4x4 2D matrix**

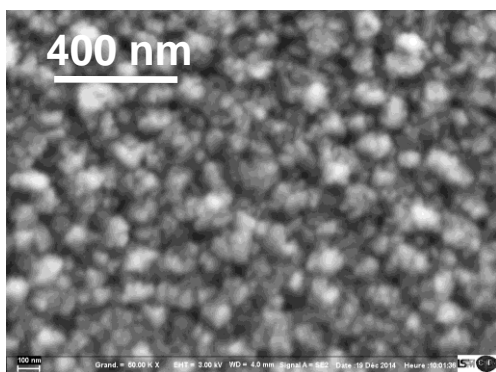
- low substrate temperature: **130 < T < 400°C**
- large area deposition: **4 inches**

\*Latrasse et al., Plasma Sources. Sci. Technol. (2007)

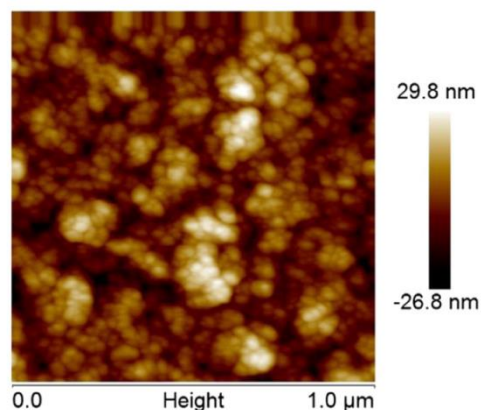
# Characteristics of NCD films grown in Plasmodie reactor

MW power	H <sub>2</sub>	CO <sub>2</sub>	CH <sub>4</sub>	T <sub>s</sub>	Pressure	Distance to the sources
3 kW	96.5 %	1 %	2.5 %	400 °C	0.35 mbar	95 mm

## Morphology

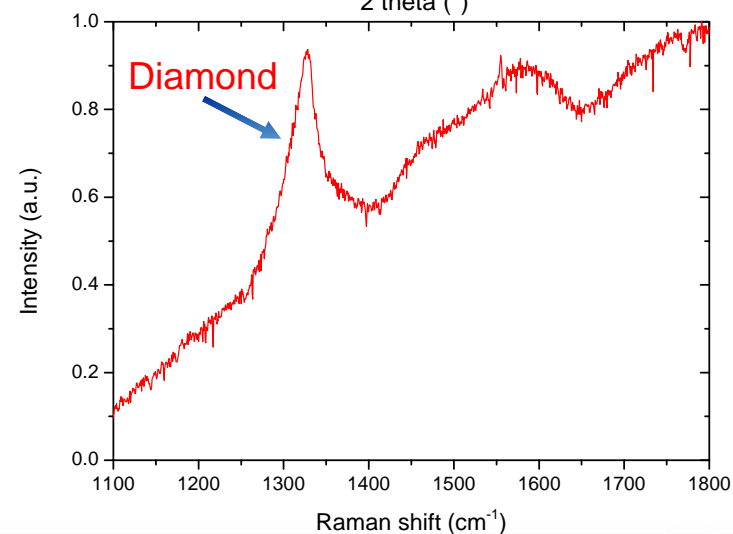
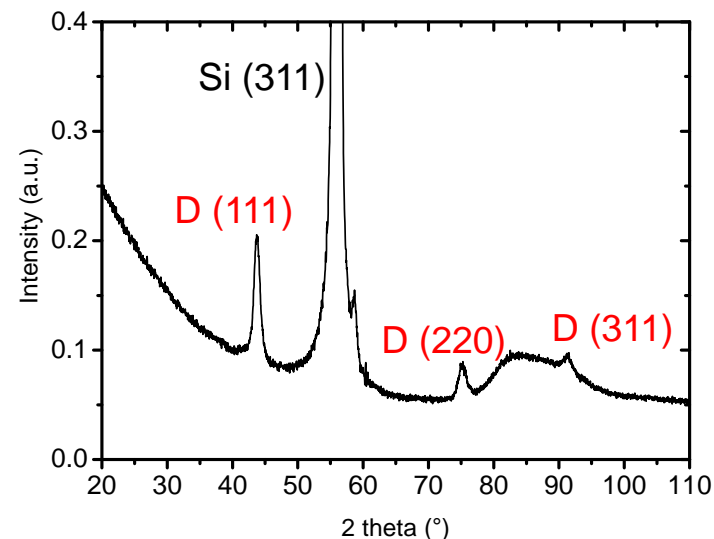


## Topography



- Ball-like aggregates
- Grain size  $\approx$  20 nm
- Roughness  $\approx$  15 nm
- Purity  $\approx$  80 % sp<sup>3</sup>
- Growth rate  $\approx$  35 nm.h<sup>-1</sup>

## Microstructure

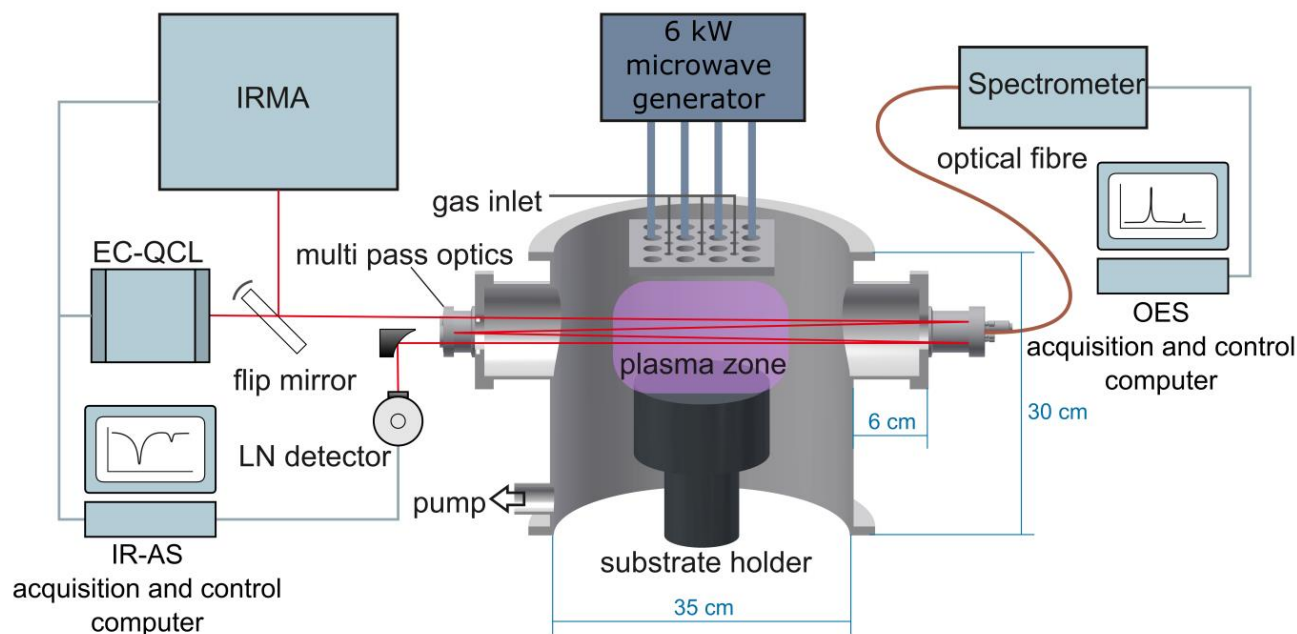




# Preliminary study of plasma

## Set up around the Plasmodie reactor \*:

\*Coll. INP Greifswald, Germany



## Optical emission spectroscopy (OES):

- Species probed in cylinder of 1.5 cm diameter

## Infrared absorption spectroscopy (IR-AS):

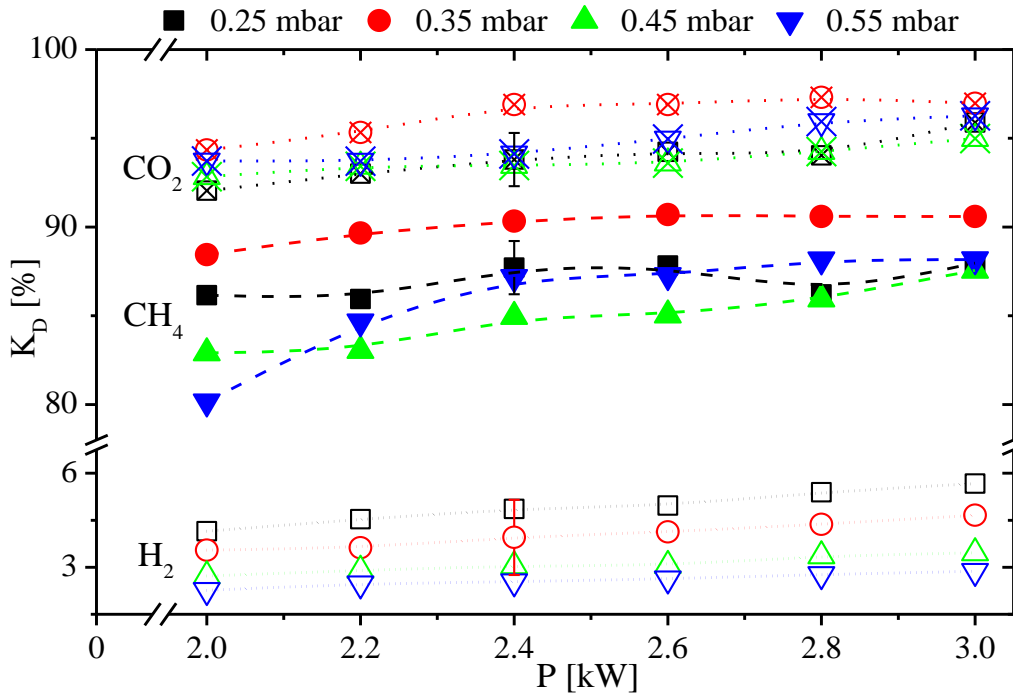
- Two kind of IR sources
  - Tunable diode lasers (TDL)
  - External quantum cascade laser (EC-QCL)

Detection of **eight** species in **excited** and **stable** states  
Determination of kinetic, rotational and vibrational temperatures  
Determination of species density

# Dissociation coefficient of gaseous precursors

<sup>1</sup> Nave *et al* PSST 2017, Part 2

## H<sub>2</sub>, CO<sub>2</sub> and CH<sub>4</sub> dissociation degrees K<sub>D</sub> 1:



- $K_D \nearrow$  when  $P_{\text{mW}} \nearrow$
- $90 \% < K_{D,\text{CO}_2} < 97 \%$
- $80 \% < K_{D,\text{CH}_4} < 90 \%$
- $2 \% < K_{D,\text{H}_2} < 6 \%$

High  $K_D$  of  $\text{CH}_4$  and  $\text{H}_2$   $\rightarrow$  Production of growth and etching species

High  $K_D$  of  $\text{CO}_2$   $\rightarrow$  Production of oxygen containing species required for growth of NCD at low  $T_s$

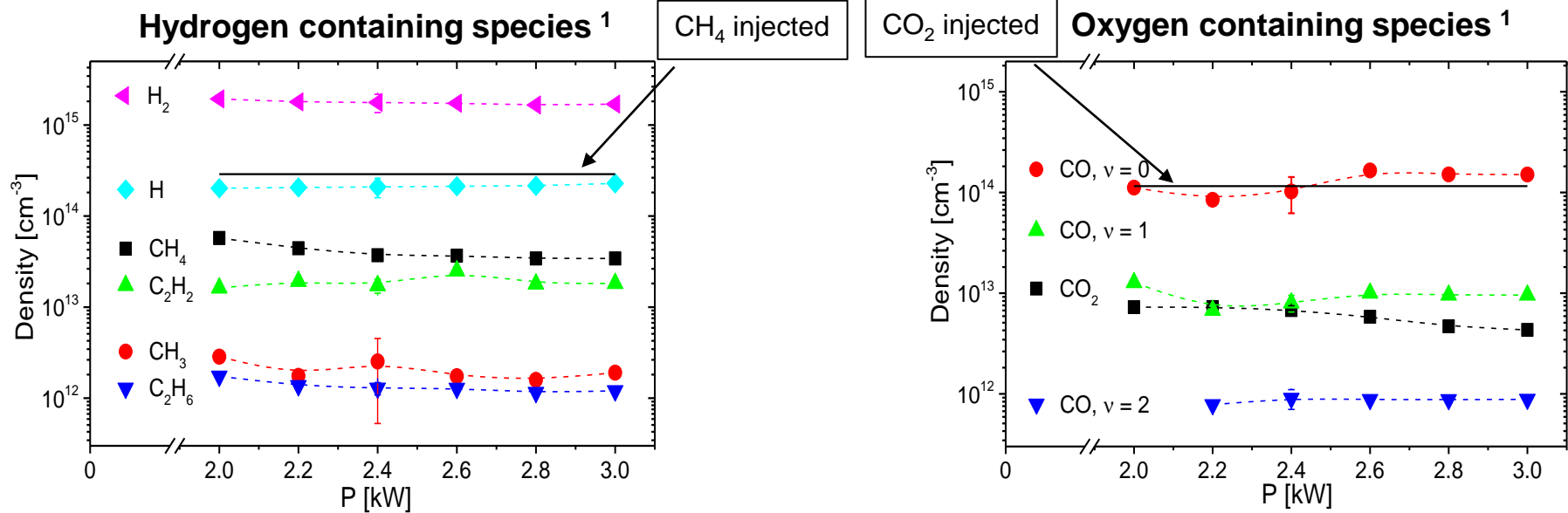
$\rightarrow$  High  $K_D$  which shows that the system is effective in terms of dissociation



# Absorption measurements : species density

**Species density as a function of  $P_{mW}$  at 0.55 mbar:**

<sup>1</sup>Nave *et al* PSST 2017, Part 2



• No high P dependency for all species

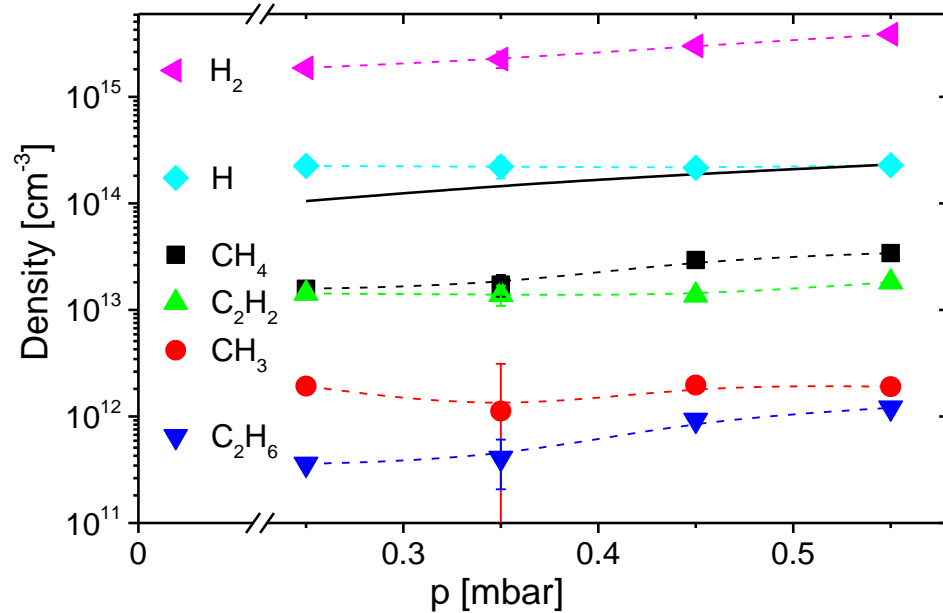
**CO and H are the main species and significant amount of CH<sub>3</sub>**

# Absorption measurements : species density

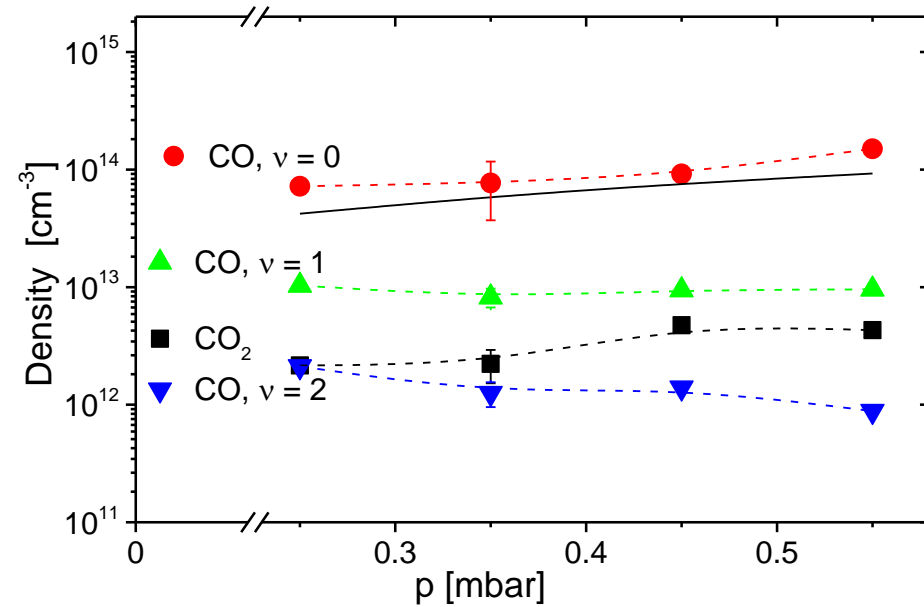
## Species density as a function of pressure at 3 kW:

<sup>1</sup> Nave *et al* PSST 2017, Part 2

### Hydrogen containing species <sup>1</sup>



### Oxygen containing species <sup>1</sup>

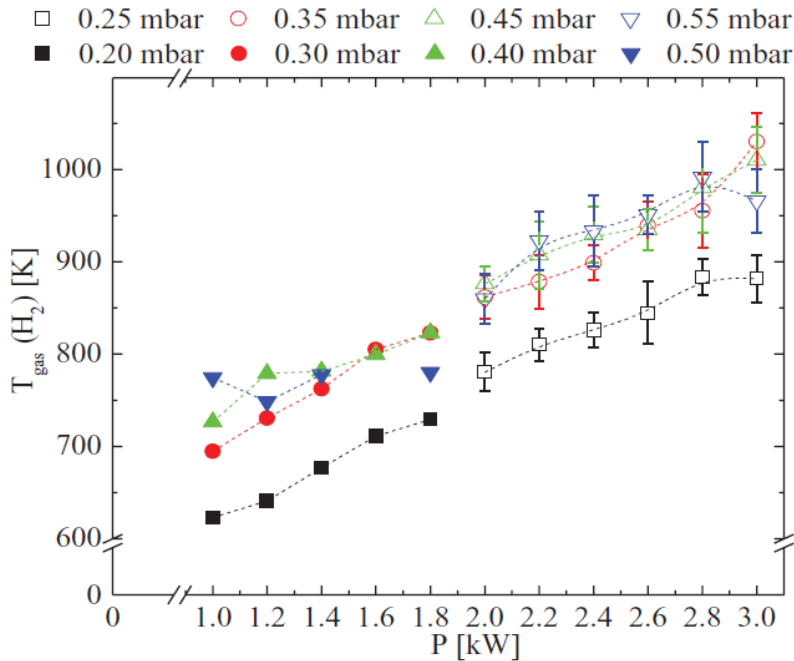


**No significant pressure dependency for all species**

# OES measurements : species temperatures

## Gas temperature $T_{\text{gas}}$ estimation\*:

**Fulcher-a system of  $\text{H}_2$  was used to  $T_{\text{rot}}$  calculation**



- $T_{\text{rot}}$   $\nearrow$  from 700 K to 1080 K when P  $\nearrow$
- At 0.25 mbar,  $T_{\text{gas}}$  ( $\text{H}_2$ ) are about 100 K lower than at higher pressures

**→** In the continuity of Rayar's results \*\*  
(12 plasma sources and  $1 < P < 1.8$  kW)

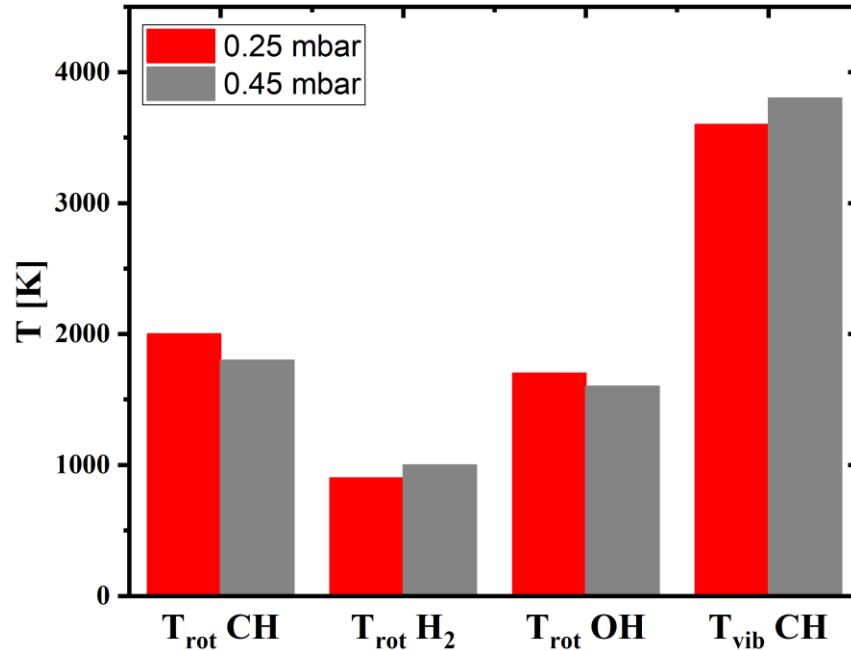
**Is  $T_{\text{rot}}$  ( $\text{H}_2$ ) really representative of gas temperature?**

\* Nave et al/PSST 2017, Part 1

\*\* M.Rayar et al., Plasma Sources Sci. Technol. (2009)

# OES measurements : species temperatures

## Temperature estimation via other species (OH, CH)



- $T_{\text{rot}} (\text{CH}) < T_{\text{vib}} (\text{CH})$  ➔ non thermal equilibrium
- $T_{\text{rot}} (\text{H}_2) < T_{\text{rot}} (\text{OH}) < T_{\text{rot}} (\text{CH})$

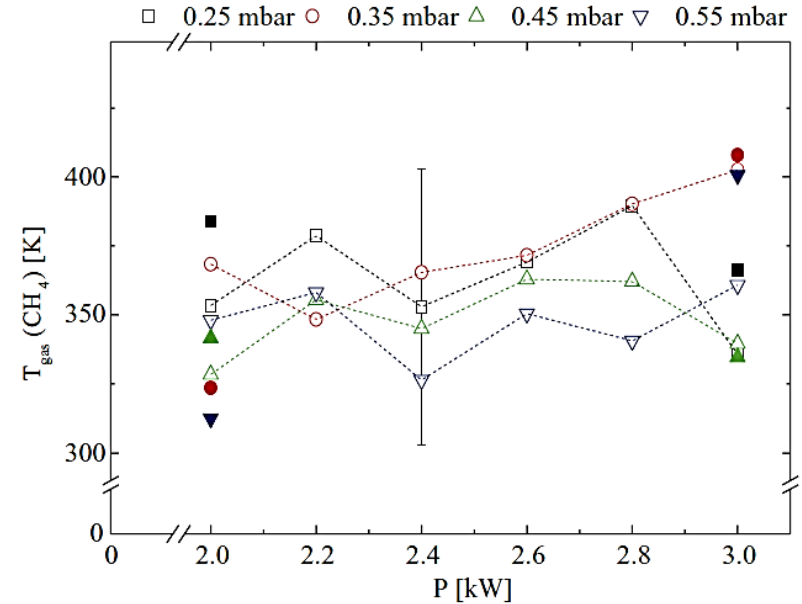
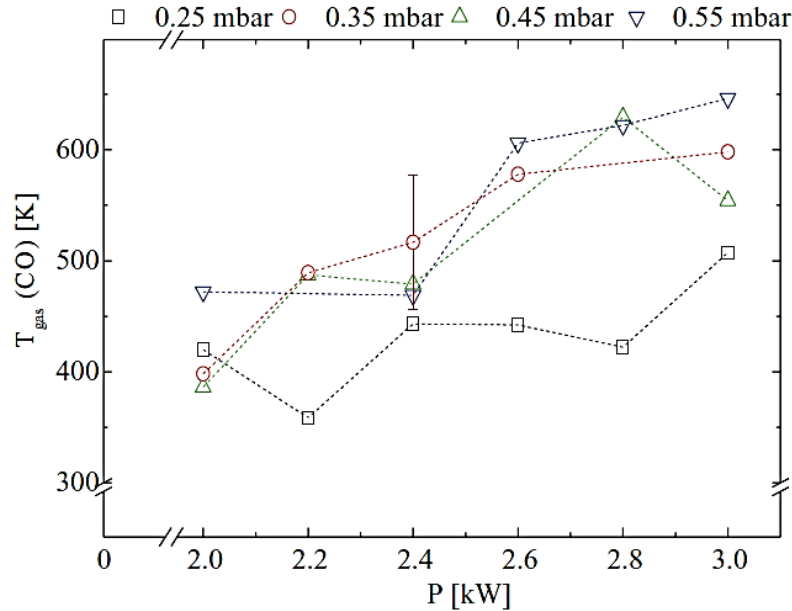
The rotational temperature depends on probed species

# Absorption measurements : species temperatures

\* Nave *et al* PSST 2017, Part 1

## Hydrogen and carbon containing species\* :

### Gas temperature determined via Doppler broadening



- $T_{\text{gas}}$  (CO)  $\nearrow$  when  $P$   $\nearrow$  (from 400 to 650 K)
- No obvious dependence of  $T_{\text{gas}}$  (CH<sub>4</sub>)  $\approx 350 \pm 50$  K

$T_{\text{gas}}$  (CH<sub>4</sub>) and  $T_{\text{gas}}$  (CO) are much lower than  $T_{\text{gas}}$  (H<sub>2</sub>)

# Summary

Species	Temperature [K]
$\text{H}_2(d^3\Pi_u^-)$	$T_{\text{rot}} = 1030 (\pm 100)$
$\text{CO}, v = 0$	$T_{\text{rot}} = 360 (\pm 30), T_{\text{kin}} = 345 (\pm 30)$
$\text{CO}, v = 1$	$T_{\text{rot}} = 525 (\pm 50), T_{\text{kin}} = 480 (\pm 50)$
$\text{CO}, v = 2$	$T_{\text{rot}} = 630 (\pm 50), T_{\text{kin}} = 635 (\pm 100)$
$\text{CO}, v = 3$	$T_{\text{rot}} = 900 (\pm 200), T_{\text{kin}} = 685 (\pm 200)$
$\text{CH}_4$	$T_{\text{kin}} = 350 (\pm 50)$
$\text{CH}_3$	$T_{\text{rot}} = 640 (\pm 180)$

Moderate pressure (0.35 mbar), intermediate position (95 mm), 3 kW

- The gas temperature depends strongly on probed zone and species

➔ Gas temperature estimated at  $600 \pm 100$  K in the plasma

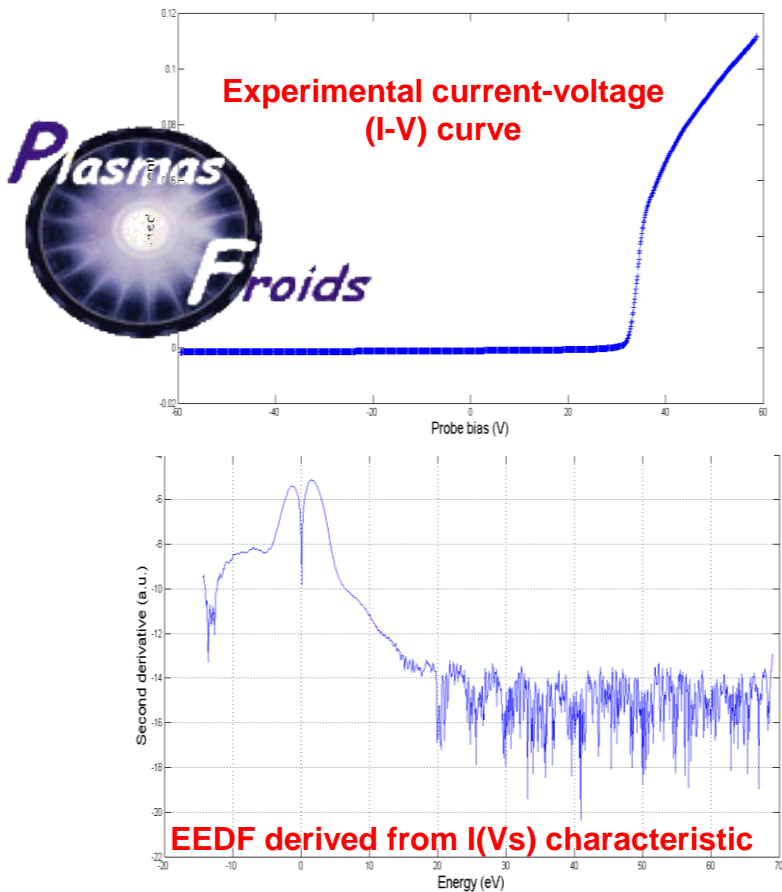
Low gas temperature ➔ Electrons play a key role in the plasma chemistry  
➔ the electron parameters should be investigated !



# Langmuir probe characteristics and EEDF

## Tools

The measuring device “QUÉ DO” provided By Réseau des Plasmas Froids



\*S.Béchu et al., Réseau plasma froid. (2014)

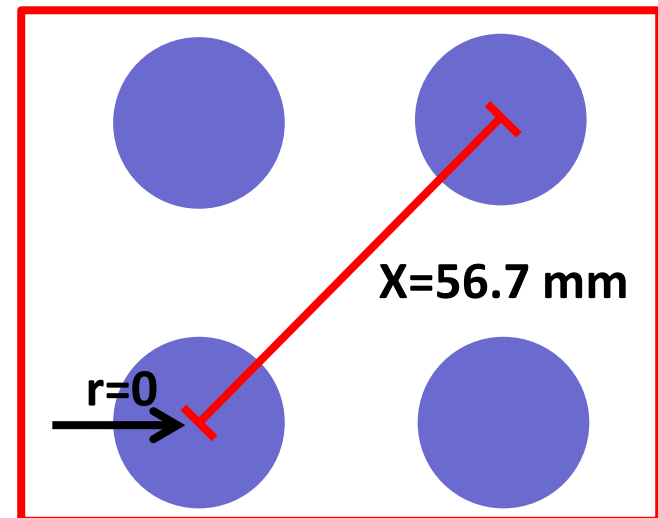
## Theory

❖ Druyvestein (1931) :  $d^2I_e/dV^2 \propto$  EEDF

$$g_e(V_s) = \frac{2m_e}{q^2 A_s} \sqrt{\frac{2qV_s}{m_e}} \frac{d^2 I_e}{dV_s^2}; n_e = \int_0^{+\infty} g_e(\varepsilon) d\varepsilon$$

$$T_{eff} = \frac{2}{3} \frac{1}{n_e} \int_0^{+\infty} \varepsilon g_e(\varepsilon) d\varepsilon; \text{ with } \varepsilon = \frac{1}{2} m_e w^2$$

## Schematic

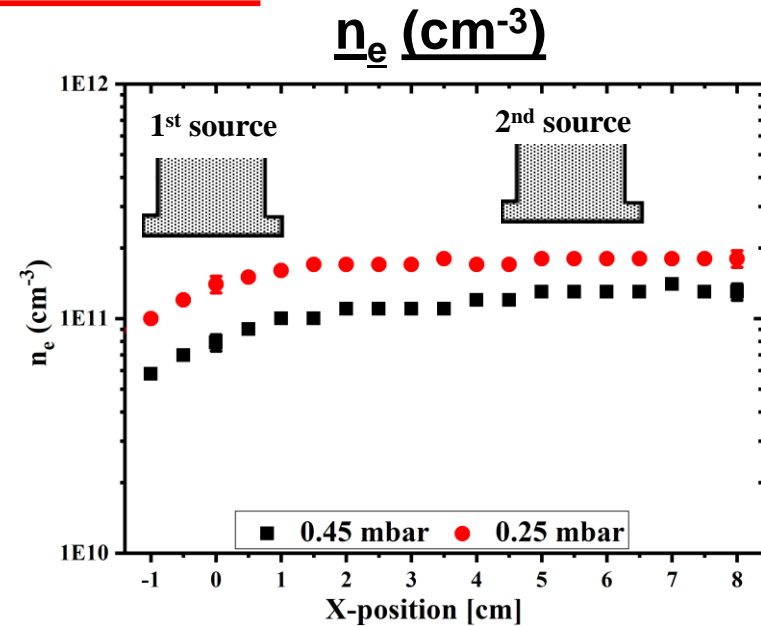
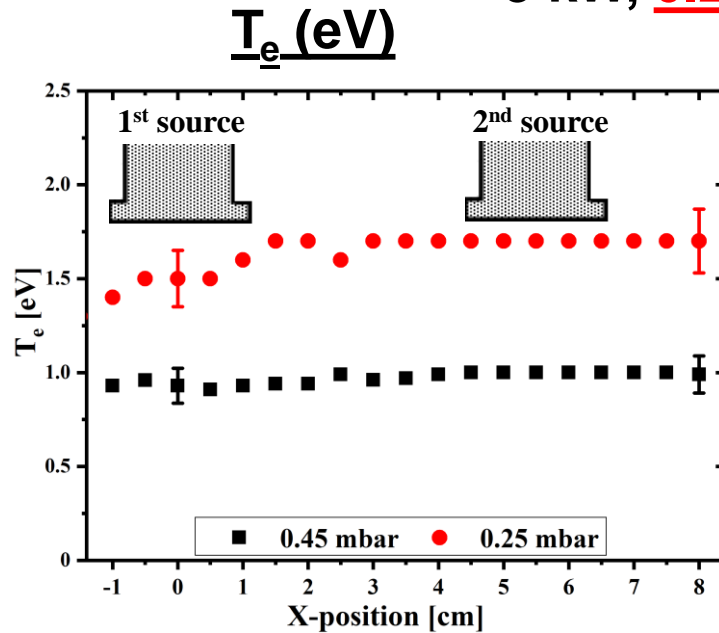


The profiles were performed at 4 cm on the diagonal of 4x4 plasma sources matrix

# Plasma features : Langmuir probe measurements

## Spatial distributions close to the MW sources

3 kW, 0.25 and 0.45 mbar



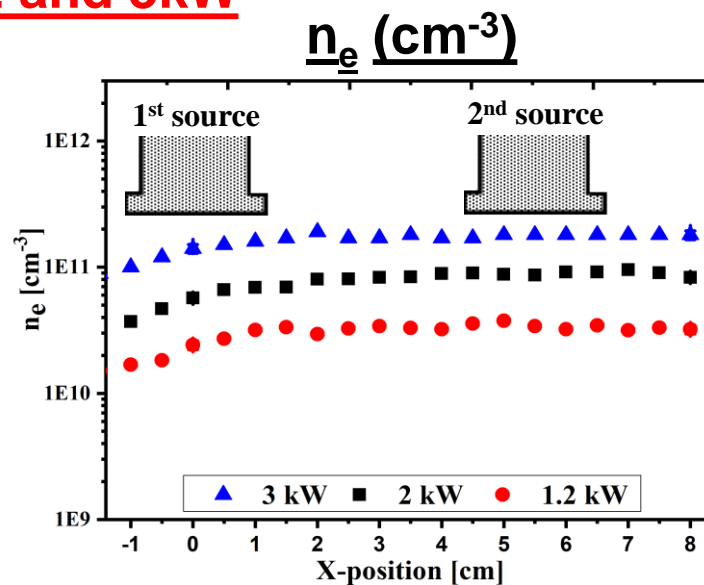
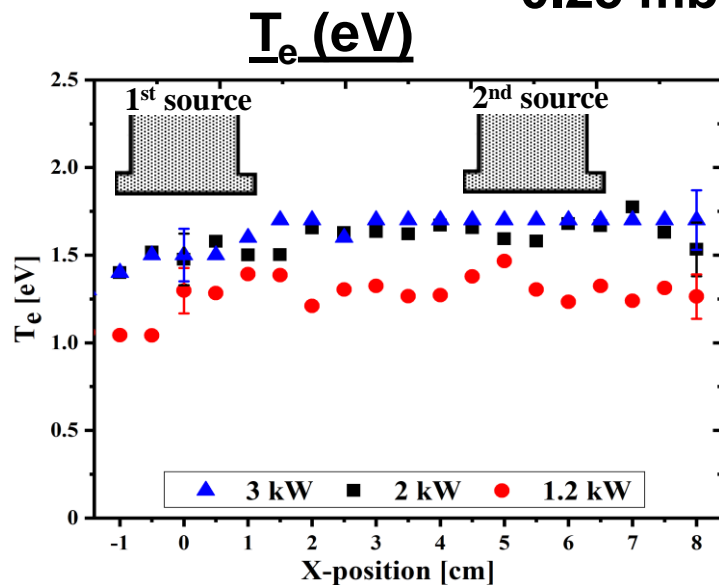
- $T_e$  and  $n_e$  are roughly constant along the diagonal (plasma between 0 and 8 cm)
- $T_e \searrow$  when  $P \nearrow$  from 1.7 to 1 eV and  $n_e \searrow$  when  $P \nearrow$  from  $2 \times 10^{11}$  to  $1 \times 10^{11} \text{ cm}^{-3}$

At higher pressure, the electrons lost more energy

# Plasma features : Langmuir probe measurements

## Spatial distributions close to the MW sources

0.25 mbar, **1.2, 2 and 3kW**



- $T_e \nearrow$  when  $P \nearrow$  from 1.2 to 1.7 eV
- $n_e \nearrow$  when  $P \nearrow$  from  $2 \times 10^{10}$  to  $2 \times 10^{11}$  cm<sup>-3</sup>
- The results at 1.2 kW and 0.25 mbar are consistent with those of Rayar\* obtained at 2 cm away from the sources plane ( $T_e=1.2$  eV,  $n_e=2.5 \times 10^{11}$  cm<sup>-3</sup>)

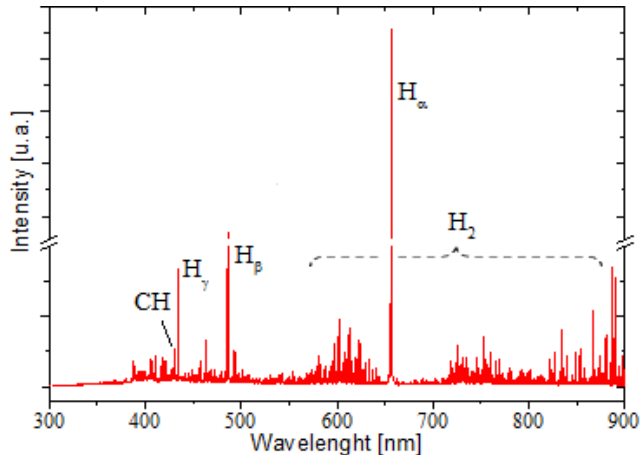


Homogeneous plasma even close to the MW sources

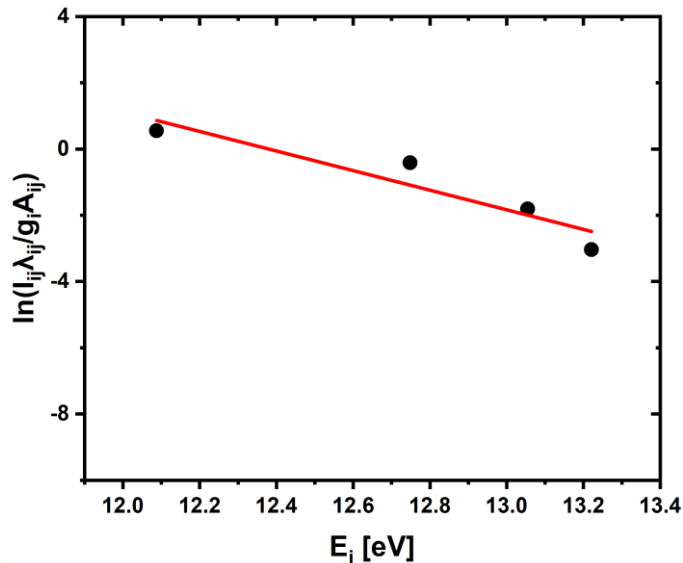
\*M.Rayar et al., Plasma Sources Sci. Technol. (2009)

# Plasma features : OES measurements

## Excitation temperature determination at 4 cm from the sources\*:



- The 4 Balmer lines of hydrogen atom (H<sub>α</sub>, H<sub>β</sub>, H<sub>γ</sub>, H<sub>δ</sub>) were used



$T_{exc}$  was determined with Boltzmann plot

$$\ln\left(\frac{I_{ij}\lambda_{ij}}{g_iA_{ij}}\right) = -\frac{E_i}{kT_{exc}} + C$$

# Plasma features : OES measurements

## Electron temperature determination:

Low temperature and low pressure plasma  $\longrightarrow$  non-equilibrium plasma

### Corona model approach\*

Equations

Methodology

Equilibrium (excitation $\leftrightarrow$ de-excitation)	$N_e N_1 k_{1i} = N_i \sum_{i>j} A_{ij},$	$\longrightarrow$	The excitation takes place only by electron impact collision and the de-excitation by spontaneous emission
Rate coefficient	$k_{1i} = b_{1i} \times e^{-E_{1i}/kT_e} \text{ cm}^3 \text{ s}^{-1},$	$\longrightarrow$	$b_{1i}$ is extracted from the fitting of $k_{1i}$
Boltzmann plot	$\ln \left( \frac{I_{ij} \sum_{i>j} A_{ij}}{h\nu_{ij} A_{ij} b_{1i}} \right) = \frac{-E_{1i}}{kT_e} + D,$	$\longrightarrow$	The inverse of the slope of the linear fitting (Boltzmann plot) gives $T_e$

\*U. Fantz., Plasma Sources Sci. Technol. (2006)

# Plasma features : OES measurements

## Electron temperature determination:

- The corona model was applied on **Balmer** lines of atomic hydrogen ( $H_\alpha$ ,  $H_\beta$ ,  $H_\gamma$ ,  $H_\delta$ )
- Several databases have been adopted based on the chosen number lines used (LXCAT, LAVROV, JANEV):

3 used lines ( $H_\alpha$ ,  $H_\beta$ ,  $H_\gamma$ )  $\longrightarrow$  LXCAT-3

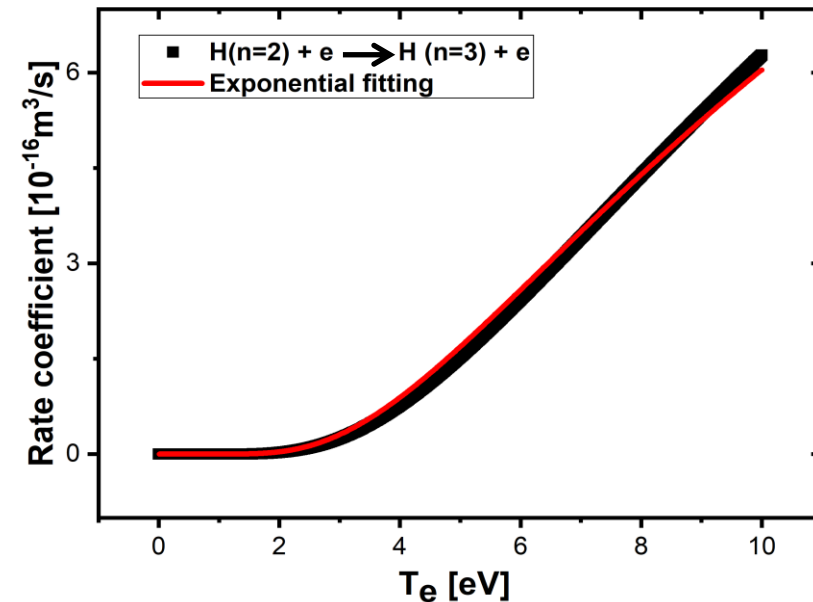
4 used lines ( $H_\alpha$ ,  $H_\beta$ ,  $H_\gamma$ ,  $H_\delta$ )  $\longrightarrow$  LXCAT and JANEV (LXCAT-4)

2 used lines ( $H_\alpha$ ,  $H_\beta$ )  $\longrightarrow$  LAVROV-1 (case 1) and LAVROV-2 (case2)

## • Rate coefficients calculated :

- ❖ From cross section obtained from LXCAT and JANEV\* databases
- ❖ By Lavrov\*\*

**Case 1:** when redistribution of populations can be neglected, **Case 2:** Boltzmann distribution of the population over the fine structure sublevels



\* R.K. Janev et al, Springer. (1987)

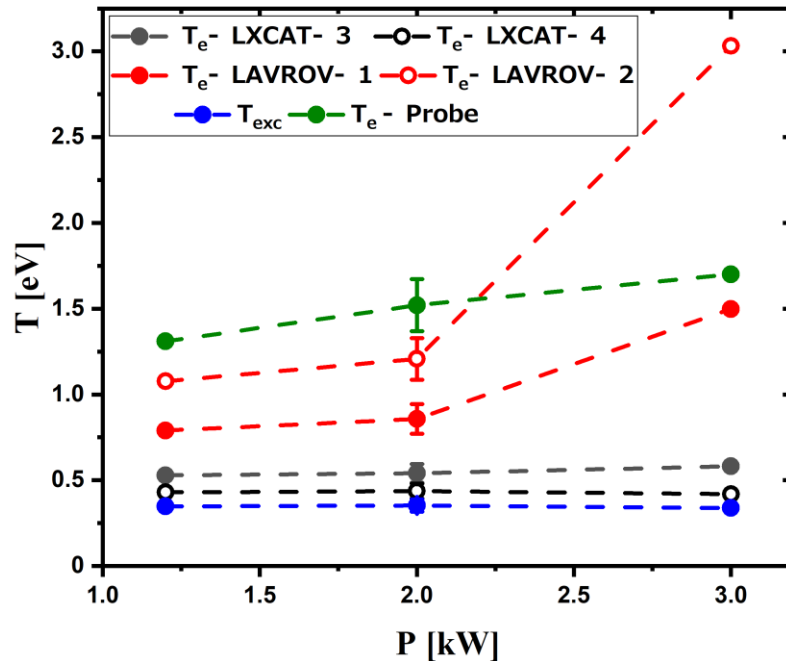
\*\*B. P. Lavrov and A. V. Pipa, *Optics and Spectroscopy*. (2002)



# Plasma features : OES measurements

## Electron temperature at 4 cm from the sources

0.25 mbar



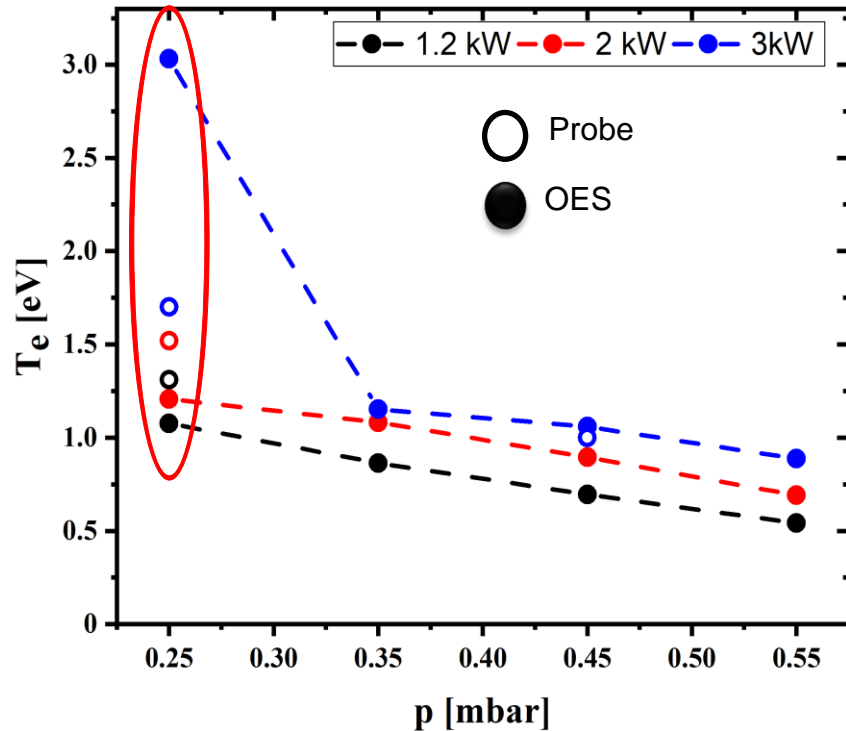
- $T_{exc}$  constant when  $P \nearrow$  ( $T_{exc} \approx 0.3$  eV)
- No tendency is observed for  $T_e$ -LXCAT as function of  $P$
- $T_e$  determined with both cases of LAVROV and probe  $\nearrow$  when  $P \nearrow$

The electron temperature depends strongly on the choice of the database

Case 2 of Lavrov is generally used for plasmas with sufficiently high particle concentrations and electric and electromagnetic (RF and microwave discharges) fields

# OES and Probe measurements

## Electron temperature at 4 cm from the sources



- $T_e$ -OES and  $T_e$ -probe  $\nearrow$  when  $P \nearrow$
- $T_e$ -OES and  $T_e$ -probe  $\searrow$  when pressure  $\nearrow$   
(At 2 kW,  $T_e$ -OES  $\searrow$  from 1.2 to 0.7 eV)
- $T_e$ -OES is close to  $T_e$  measured by the probe:

At 0.25 mbar and 2 kW,  $T_e$ -OES = 1.2 eV  
and  $T_e$ -probe = 1.5 eV

$T_e$  -OES is in well accordance with  $T_e$ - probe **only if** case 2 of Lavrov is used as database

# Plasma modelling

## Two-dimensional self-consistent plasma model for hydrogen\*

### Electromagnetic module

Maxwell's equations

$$\mu_0 \frac{\partial \mathbf{H}}{\partial t} = - \nabla \times \mathbf{E}$$

$$\varepsilon_0 \frac{\partial \mathbf{E}}{\partial t} = \nabla \times \mathbf{H} + en_e \mathbf{v}_e$$

Coupling with  $n_e$  and  $\mathbf{v}_e$

Coupled with electron momentum equation

$$\frac{\partial \mathbf{v}_e}{\partial t} + \nu_m \mathbf{v}_e = - \frac{e}{m_e} \mathbf{E}$$

Collision frequency

Time-averaged absorbed microwave power

$$P = -C \frac{en_e \omega}{2\pi} \int_0^{2\pi/\omega} \mathbf{v}_e \cdot \mathbf{E} dt$$

→  $\mathbf{E}, \mathbf{H}, \mathbf{v}_e, P$

\*Hagelaar et al., J. Appl. Phys. (2004)

# Plasma modelling

## Plasma module

### - Species continuity equations

$$-\nabla \cdot (D_s N \nabla x_s) = S_s \quad \rightarrow \quad \text{Plasma composition } (n_s, x_s)$$

Diffusion      Plasma chemistry

### - Electron energy equation

$$\nabla \cdot (\Gamma_e \frac{5}{2} k_B T_e - \lambda_e \nabla T_e) = P - Q \quad \rightarrow \quad \text{Electron temperature } (T_e)$$

Absorbed microwave power

Electron flux      Electron conductivity      Energy transfer through collisions

### - Heavy species energy equation


$$\nabla \cdot \left( \sum_s \Gamma_s (C_s T + H_{0,s}) - \lambda \nabla T \right) = Q - Q_{\text{rad}} \quad \rightarrow \quad \text{Gas temperature } (T_g)$$

Particle flux      Conductivity      Radiative loss

### - Offline Boltzmann solver $\rightarrow$ Reaction rate coefficients $k_m(T_e)$

### - Simple chemistry : 8 species ( $\text{H}_2, \text{H}, \text{H}^*, \text{H}^{**}, \text{H}^+, \text{H}_2^+, \text{H}_3^+, \text{e}$ ) linked by 34 reactions

# Conclusions

- ✓ Temperatures depend strongly on the probed species
- ✓ Gas temperature of the plasma estimated at  $600 \pm 100$  K  low gas temperature which permits to grow NCD films at  $T_s$  below  $400$  °C
- ✓ Since low temperature plasmas as a rule are non-Maxwellian, the determination of electron parameters from EEDF measurement is recommended
- ✓ plasma is homogeneous close to the microwaves sources
- ✓  $T_e$  can be determined by OES and have values close to those measured with the probe **only if** **The coronal approximation is adopted and** case 2 of Lavrov is used as database
- ✓ Both the experimental and modelling values of electrons parameters are in well accordance

## Work in progress:

- Determination of  $T_e$  by using argon lines
- Atomic hydrogen estimation by actinometry

# Acknowledgements

- **LPSC-CNRS-IN2P3, Grenoble**

A. Lacoste, J. Pelletier

- **INP, Greiswald**

J. Röpcke, B. Baudrillart, A. Nave, S. Hamman, J.H. van Helden

**Financial supports:**

ANR-11-LABX-086, ANR-11- IDEX-0005-02, BQR Université Paris 13, ADAM Labex project, French-Germany Procope Project